DESIGN OF AUXETIC SANDWICH PANELS FOR STRUCTURAL APPLICATIONS

Li Yang[1], Ola Harrysson[2], Denis Cormier[3], Harvey West[2], Chun Park[2], Kara Peters[2]

[1]University of Louisville, Louisville, KY
[2]North Carolina State University, Raleigh, NC 27695
[3]Rochester Institute of Technology, Rochester, NY 14623

Abstract

Based on an analytical modeling analysis, a sandwich structure with a 3D re-entrant auxetic core was designed. Auxetic samples were produced by electron beam melting (EBM) and selective laser sintering (SLS), and compared to other regular cellular sandwich structures through various experiments. It was shown that sandwich structures with pre-designed auxetic cores could exhibit significantly improved mechanical properties such as bending compliance and energy absorption, which are critical to many structural applications. This work demonstrated an alternative of effectively designing 3D cellular structures, and also showed the potential of this type of auxetic structure in applications via careful design.

Introduction

In many applications, the sandwich structures are often subject to conflicting requirements such as the need for minimal weight versus the need for high stiffness [1]. Two-dimensional cellular structures and stochastic foams are predominantly used as sandwich cores, but they often lack the level of properties that satisfy all requirements [2-6]. Three-dimensional cellular structures possess many advantages in such applications. However, their practical use is largely hindered by the restrictions of manufacturing processes and the resulting limitation in the development of design theories [6-10].

One such three dimensional structure that shows potential is the auxetic structure, or a structure that exhibits negative Poissons' ratio in one or more directions. Due to their counterintuitive behavior and exceptional properties, auxetic structures have received considerable attention in past years [11-20]. The combination of high shear modulus and strength [11-12], high toughness [13-16], large bending compliance [17] as well as tailorable elastic modulus and yield strength [18-20] makes auxetic structures especially suitable for sandwich structure applications.

Traditionally, auxetic structures have been fabricated via a multi-step process that involves rather complex designs of molds and heat compression processes [11]. Furthermore, the mechanical properties of the resulting structures are largely empirical. Additive manufacturing provides an efficient alternative to fabricate these structures. In combination with design theory, additive manufacturing processes could be implemented to produce functional sandwich parts via design for functionality (DFF).

In the current paper, a 3D re-entrant auxetic structure was investigated. Previous work has established analytical models for some fundamental properties of the re-entrant auxetic structure, and it was shown that the mechanical properties of this type of structure could be tailored to a wide range of different applications [18-22]. Based on this work, this paper demonstrates the design of the re-entrant auxetic structure for sandwich panel applications with the focus of bending compliance and energy absorption abilities. An experimentally based study was carried out to compare two re-entrant auxetic sandwich structures to conventional sandwich structures with non-stochastic cellular cores, and the results demonstrate the feasibility of using auxetic structure for such applications.

Structural designs

Fig. 1(a) shows the unit cell design of the 3D re-entrant auxetic structure. This auxetic structure is an orthotropic structure where directions *x* and *y* exhibit identical properties due to the cell's symmetry. Therefore, the design of the structure could be represented by the simplified 2D geometry shown in Fig.1(b), which includes the length of the vertical (*H*) and re-entrant (*L*) struts, the re-entrant angle *θ*, and the thickness (*t*) of the strut (not shown in the figure).

a. Unit cell   b. Design parameters
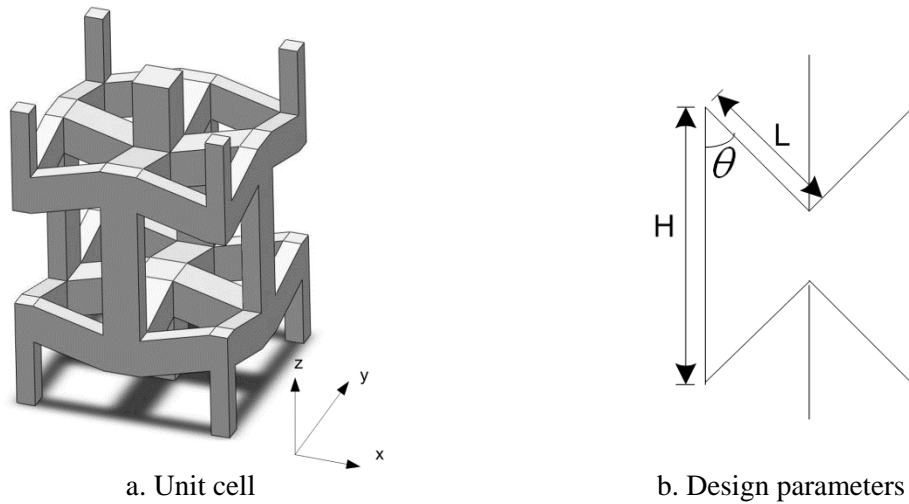
Figure 1 Design of the 3D re-entrant cellular structure

It has been shown that various mechanical properties including Poisson's ratio, modulus and yield strength of the 3D re-entrant auxetic structure can be determined by the geometrical design parameters and solid material properties, as shown in Eq.(1)-(6) [19-22].

$$v_{zx} = -\frac{(\frac{L^2}{Et^2} + \frac{6}{5G})\cos\theta(\alpha - \cos\theta)}{\frac{L^2\sin^2\theta}{Et^2} + \frac{6\sin^2\theta}{5G} + \frac{4\alpha}{E}} \quad (1)$$

$$v_{xz} = -\frac{\sin^2\theta}{\cos\theta(\alpha - \cos\theta)} \quad (2)$$

$$E_z = \cfrac{(\alpha - \cos\theta)}{\cfrac{2\alpha L^2 \sin^2\theta}{Et^2} + \left(\cfrac{L^4}{2Et^4} + \cfrac{3L^2}{5Gt^2}\right)\sin^4\theta} \qquad (3)$$

$$E_x = \cfrac{1}{L^2\cos^2\theta(\alpha-\cos\theta)} \cdot \cfrac{1}{\left(\cfrac{L^2}{2Et^4}+\cfrac{3}{5Gt^2}\right)} \qquad (4)$$

$$\cfrac{\left(\sigma_Y^2 - \cfrac{9\sigma_z^2 L^4\sin^6\theta}{16t^4}\right)t^3}{4\sigma_Y} - \cfrac{4\sigma_z^2 L^4\sin^4\theta\cos^2\theta\sigma_Y}{\left(64\sigma_Y^2 - \cfrac{36\sigma_1^2 L^4\sin^6\theta}{t^4}\right)t} = \cfrac{2L^3\sin^3\theta}{8}\sigma_z \qquad (5)$$

$$\cfrac{\left(\sigma_Y^2 - \cfrac{9L^4(\alpha-\cos\theta)^2\sin^2\theta\cos^2\theta\sigma_x^2}{16t^4}\right)t^3}{4\sigma_Y} - \cfrac{16L^4\left(\cfrac{\cos^4\theta}{\sin^2\theta}+4\right)(\alpha-\cos\theta)^2\sin^2\theta\sigma_Y\sigma_x^2}{\left(256\sigma_Y^2 - \cfrac{144L^4(\alpha-\cos\theta)^2\sin^2\theta\cos^2\theta\sigma_x^2}{t^4}\right)t} = \cfrac{L^3(\alpha-\cos\theta)\sin\theta\cos\theta\sigma_x}{4}$$

$$(6)$$

In Eq.(1)-(6), E, G, and σ_Y are the elastic modulus, shear modulus and yield strength of the solid material, respectively. $\alpha = H/L$, and v_{zx}, v_{xz}, E_z, E_x, σ_z, σ_x are the Poisson's ratios, modulus and yield strength of the re-entrant auxetic structure in the z and x directions, respectively. Note that Eq. (5) and Eq. (6) are in implicit form of the yield strength in the respective directions. Though not shown here, from Eq. (1)-(6) it could be derived that the mechanical properties of the re-entrant auxetic structure have a monotonous relationship with respect to its Poisson's ratio. In general, the mechanical properties of the re-entrant auxetic structure improve with larger negative Poisson's ratio. While in agreement with previous experimental observations using stochastic auxetic structures, this relationship also provides an efficient method for quick screening of designs of re-entrant auxetic structures, along with the relative density relationship derived for general cellular structures [23]. After screening the design, a more detailed analysis through either analytical methods or more accurately, finite element analysis, can be carried out to fine tune the designs [19-22].

In many applications of sandwich panel structures, the structure is required to withstand large amounts of bending/shearing deflection while maintaining sufficient stiffness. In addition, when such structures are used in aerospace and automobile applications as exterior surfaces, low-energy impact protection from small objects and debris is also an important factor for consideration. Auxetic structures were predicted to possess promising properties in these applications compared to regular cellular structures. Based on the analytical model, it becomes possible to design a 3D auxetic structure that meets both requirements. In this study, the bending performance and low-impact energy absorption ability of the auxetic structures were evaluated in separate sets of experiments.
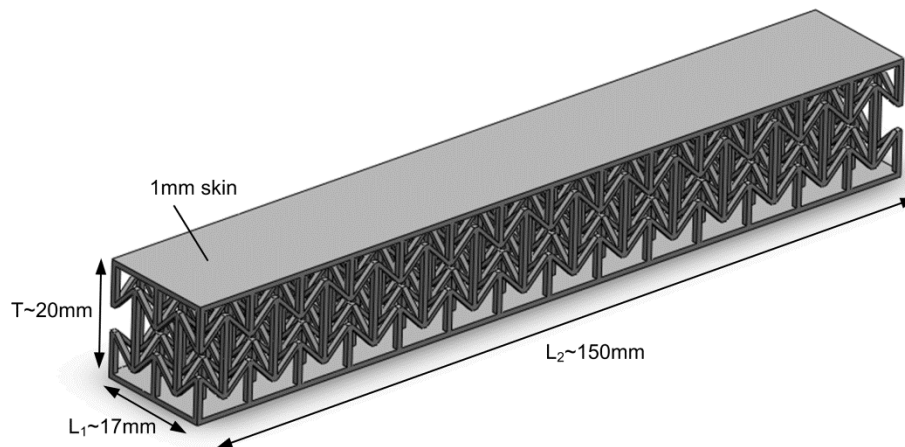
Bending performance

Considering the fact that the Poisson's ratio values can be used as a performance indicator for different designs, two re-entrant auxetic unit cell structures were designed with significantly different Poisson's ratio values. As shown in Table 1, auxetic structure A1

possesses a larger negative Poisson's ratio value in v_{zx} while auxetic structure A2 possesses larger negative Poisson's ratio value in v_{xz}. Due to the way the 3D CAD model was created, the thickness of the vertical strut t_V differs from that of the re-entrant strut t_R for each design.

Table 1 Design parameters of auxetic structures for bending performance

Design	H (*mm*)	L (*mm*)	θ (Deg.)	t_V (*mm*)	t_R (*mm*)	v_{zx}	v_{xz}	Relative Density
A1	15	7.5	45	1	0.707	-1.704	-0.547	0.063
A2	7.595	4	70	1	0.940	-0.445	-1.659	0.116

The sandwich panels for bend testing were designed as illustrated in Fig. 2 using the two auxetic core designs (A1 and A2). The dimensions of the sandwich panel cores were kept at approximately 17 *mm* x 20 *mm* x 150 *mm* while maintaining structural symmetries in each direction. In addition, the thickness of the sandwich skins was also fixed at 1 mm in the design. The resulting structures had 1 x 2 x 14 unit cell repetitions for design A1, and 1.5 x 2 x 20 unit cell repetitions for design A2.
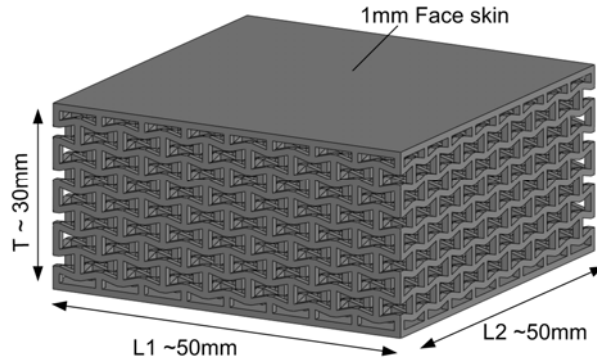

Figure 2 Sandwich panel with auxetic core for bending evaluation

Low energy impact performance

The samples for low energy impact performance were designed in a similar manner. Two re-entrant auxetic designs with significantly different Poisson's ratios in all directions, A3 and A4, were constructed using parameters shown in Table 2. The dimensions of the sandwich cores were kept at around 55 x 55 x 30 mm while maintaining structural symmetries in each direction, as shown in Fig. 3.

Table 2 Design parameters of auxetic structures for low energy impact performance

Design	H (mm)	L (mm)	θ (Deg.)	t_V (mm)	t_R (mm)	v_{zx}	v_{xz}	Relative Density
A3	4	3.75	75	1	0.966	-0.180	-4.462	0.211
A4	7.5	3.75	45	1	0.707	-1.343	-0.610	0.220

Figure 3 Sandwich structure with auxetic core for low energy impact performance

Experimentation

The sandwich samples for bending performance were manufactured via the electron beam melting (EBM) process using 100/+325 mesh spherical Ti-6Al-4V powder produced by the plasma rotating electrode process (PREP). Identical default process settings for electron beam melting of lattice geometries were used to produce all samples. All samples were oriented in the build chamber such that the two skin faces were normal to the build direction. Three samples were made for each type of structure, and the samples were fabricated in two builds.

The sandwich samples for the low energy impact performance were produced by Fineline Prototyping Inc. using a 3D Systems SinterStation Pro selective laser sintering (SLS) system with ALM PA650 powder. All samples were built in the same orientation with the face sheets normal to the build direction. Six samples were made for each type of structure. After the samples were made, they were cleaned in the standard powder recycling system for this process.

After the samples were cleaned, their dimensions were measured using digital calipers, and their masses were weighed using a digital balance having a resolution of 0.0001g. Tables 3 and 4 show the actual dimensions of the sandwich samples for bending and impact testing respectively. The dimensional accuracy of the samples for both tests was within ±5% compared with the CAD model. It is worth noting that due to the noticeable stair step effect observed with the auxetic samples, the strut sizes of the auxetic cores for A3 and A4 sandwich samples were only about 75% of the designed values.

**Table 3 Actual sample dimensions for bend testing**

Design	L_1 (mm)	L_2 (mm)	T (mm)	Rel. Dens.
A1	20.405±0.259	148.675±0.155	22.538±0.125	0.149±0.008
A2	19.829±0.153	150.334±0.140	16.222±0.029	0.214±0.006

**Table 4 Actual sample dimensions for low energy impact testing**

Design	L_1 (mm)	L_2 (mm)	T (mm)	Rel. Dens.
A3	68.449±0.057	68.457±0.025	26.467±0.051	0.226±0.006
A4	53.971±0.054	53.962±0.035	30.709±0.016	0.175±0.003

The bending performance was evaluated by three-point bend testing as shown in Fig. 4. The testing was performed on an Applied Test System 1620C at a constant strain rate of 1.27 mm/min. The span of the support points was 114.3 mm. The support rollers had a diameter of 12.7 mm, and the load roller had a diameter of 25.4 mm.

The low energy impact performance was evaluated by the drop weight test as shown in Fig. 5. The testing was performed on a drop weight tester with the same setup used by a different study [24]. The drop impactor and the cross head weighed 5.5 kg in total, and the diameter of the impactor's hemispherical probe was 19 mm. The samples were clamped between two clamping plates, and the impactor dropped down from a pre-marked height and impacted the samples. The impact energy level used for these tests was between 1-1.3 J (e.g. initial impact velocity 0.6 m/s-0.7 m/s), and the impact was repeated for up to five times for each sample except for the cases where the top skin of the samples were completely perforated.
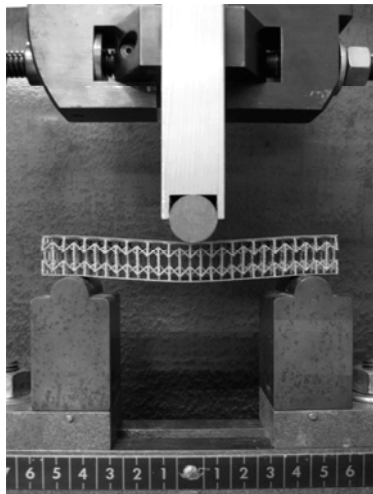
Figure 4 Three-point bend test
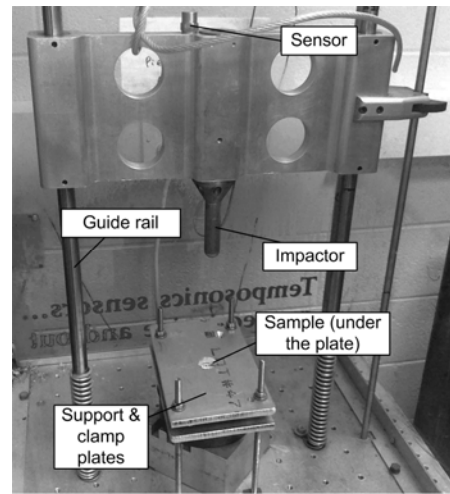
Figure 5 Drop weight low energy impact test

Bend Test Results

Table 5 shows the results of the three-point bend testing for different structural designs. From Table 5 it can be seen that the two auxetic sandwich structures exhibit significantly different properties. The auxetic sandwich A1 exhibits significantly lower bending stiffness and

higher bending compliance compared with auxetic structure A2. From Table 1, it is known that the auxetic structure A2 has a larger negative Poisson's ratio v_{yx}, so it is expected to exhibit significantly higher flexural stiffness as well as maximum allowable loading compared to auxetic structure A1. As a result, it is also expected that sandwich panel A2 would exhibit higher total energy absorption at fracture, which in practice can be interpreted as a measurement of the structural toughness. On the other hand, auxetic sandwich A1 exhibits significantly higher resilience compared to A2 with approximately 50% more maximum deflection. This also contributes to the total energy absorption of the A1 sandwich samples. Furthermore, it was observed that the auxetic sandwich samples did not exhibit any localized stress concentration at the loading point. This could be largely attributed to the negative Poisson's ratio values of the auxetic cores, which accommodate compressive stress by lateral shrinkage, thereby minimizing the stress concentration and skin wrinkling at the loading point, as can be observed in Fig. 4.

Table 5 Bending performance of different structural designs

| Design	Max. Force (N)	Max. Deflection (mm)	Flexural Stiffness ($N\text{-}m^2$)	Max. Energy Abs. (J)
A1	1206.43±37.35	9.20±0.77	4.10±0.33	8.73±0.50
A2	3432.23±58.58	5.96±0.27	17.93±0.80	16.54±1.61

Low Energy Impact Test Results

Fig. 6 shows the average total energy absorption and energy absorption per strike for auxetic structures A3 and A4. During the test, each auxetic A4 sandwich sample was perforated after 3 strikes. In the application of low energy impact protection, it is highly desired that the protection structure absorb as much energy as possible at a minimum response force level in order to minimize the impact to the structures being protected. Therefore, the auxetic A4 sandwich exhibited a very desirable combination of high energy absorption and low peak response force that would make it an ideal candidate for such application. Since the auxetic A4 design has a significantly higher negative Poisson's ratio v_{zx} in the impact direction, it could be expected that the A4 sandwich would exhibit higher strength as well as modulus, which in general indicate higher total energy absorption for cellular structures.

It is often the case with additive manufacturing processes that material properties exhibit a certain degree of anisotropy. This can be a significant factor for thin features such as cellular struts. It was expected that the sandwich samples were weakened as a result of the specific build direction. Tensile tests were therefore performed on coupons fabricated in three orientations (0°, 45°, and 90°) with respect to the vertical build axis in order to provide an estimation of the anisotropy of the parts. Fig. 8 shows the relationships of the mechanical properties of the structures based on the build orientation. Through simple analysis it is known that the auxetic A4 sandwich sample struts had the smallest build orientation angle (i.e. the angle between the strut axis and the build direction). Therefore, it could be expected that the A4 samples were further weakened by another 20-30% due to the strut orientation. When considering the fact that the auxetic samples were weakened due to the reduced core strut size, it is reasonable to conclude

that the auxetic A4 design with the large negative Poisson's ratio would result in significantly improved low energy impact protection.

As a conclusion, it could be seen that through efficient design screening, the auxetic sandwich structures could be designed to meet the specific needs of different applications. In the case of applications with multiple objectives, an optimization method could be implemented to achieve a good balance between design extremes. For example, in this study, it is shown that in general, the bending performance and the impact energy absorption are two conflicting requirements for auxetic sandwich structures. Therefore in order to design structures that meet both requirements, weighing factors will need to be chosen, and a compromise solution will be achieved to satisfy design requirements.
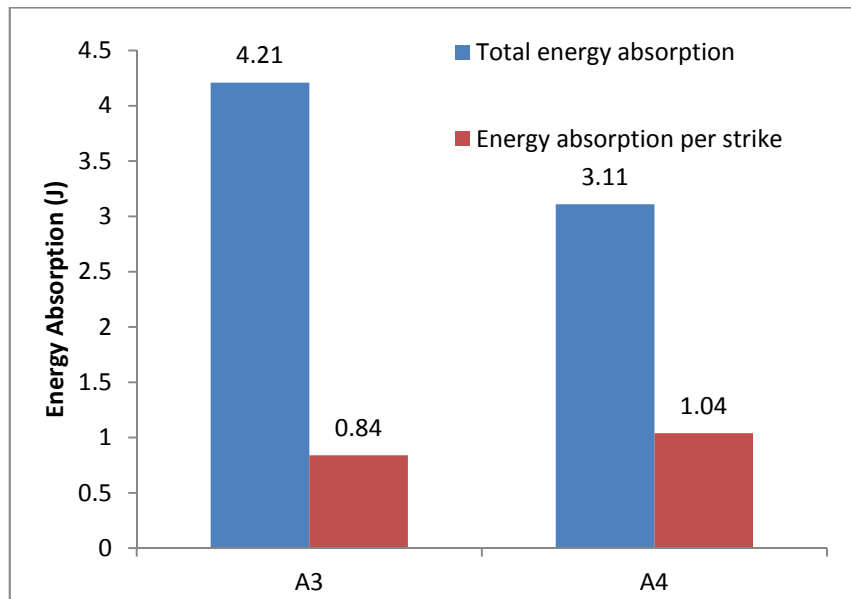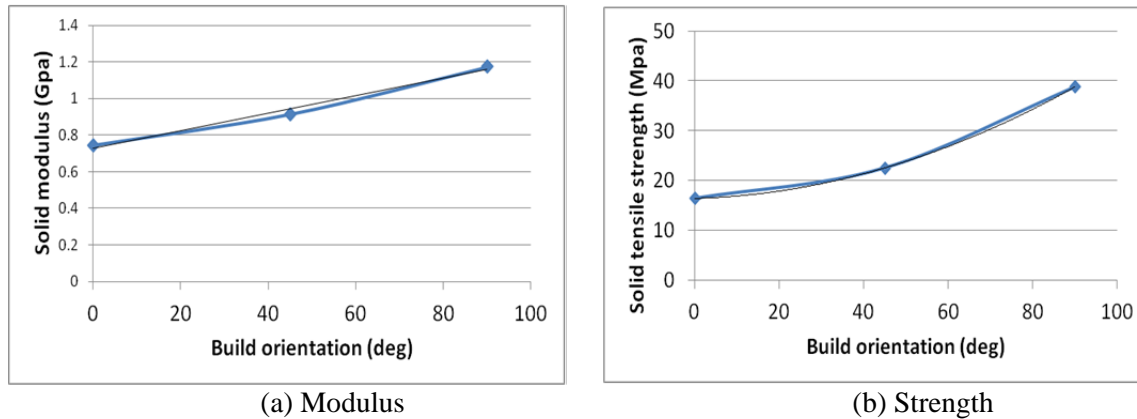

Figure 6 Total energy absorption and average energy absorption for various sandwich designs
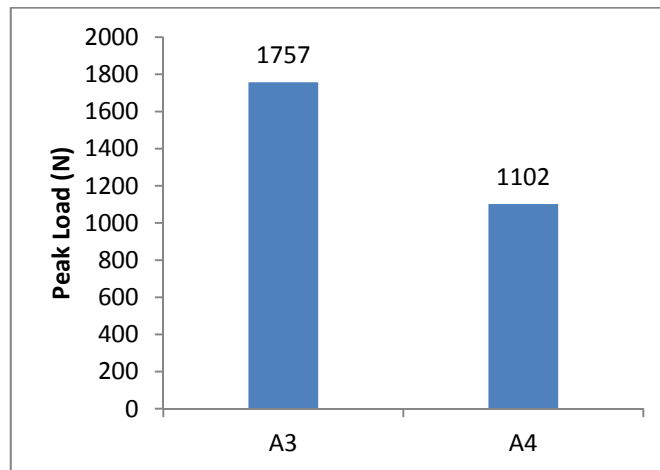
Figure 7 Peak response force for various sandwich designs

| (a) Modulus | (b) Strength |

Figure 8 Anisotropy of the parts made in SLS

Conclusion

In this study the bending performance and low energy impact performance of auxetic sandwich structures were assessed. It was observed that through design the auxetic sandwich structures could exhibit significantly varied performance in each application cases. Further work that applies optimization to the analytical model for multi-objective designs could be done on the basis of the current work, and could potentially make significant contribution to the development of design for additive manufacturing (DFAM) theories.

Reference

[1] H.G. Allen. Analysis and design of structural sandwich panels. Pergamon Press, Oxford, UK. 1969.

[2] T.M. McCormack, R. Miller, O. Kesler, L.J. Gibson. Failure of sandwich beams with metallic foam cores. International Journal of Solids and Structures. 38(2001): 4901-4920.

[3] Gaetano G. Galletti, Christine Vinquist, Omar S. Es-Said. Engineering Failure Analysis. 15(2008): 555-562.

[4] V. Crupi, R. Montanini. Aluminum foam sandwiches collapse mods under static and dynamic three-point bending. International Journal of Impact Engineering. 34(2007): 509-521.

[5] A. Petras, M.P.F. Sutcliffe. Failure mode maps for honeycomb sandwich panels. Composite Structures. 44(1999): 237-252.

[6] H.J. Rathbun, F.W. Zok, A.G. Evans. Strength optimization of metallic sandwich panels subject to bending. International Journal of Solids and Structures. 42(2005): 6643-6661.

[7] Gregory W. Kooistra, Douglas T. Queheillalt, Haydn N.G. Wadley. Shear behavior of aluminum lattice truss sandwich panel structures. Materials Science and Engineering A. 472(2008): 242-250.

[8] V.S. Despande, N.A. Fleck. Collapse of truss cores sandwich beams in 3-point bending. International Journal of Solids and Structures. 38(2001): 6275-6305.

[9] Sung-il Seo, Jung-Seok Kim, Se-Hyun Cho, Seong-Chul Kim. Manufacturing and mechanical properties of a honeycomb sandwich panel. Materials Science Forum. 580-582(2008): 85-88.

[10] M. Hostetter, B. Cordner, G.D. Hibbard. Stochastic honeycomb sandwich cores. Composites: Part B. 43(2012): 1024-1029.

[11] R. Lakes. Foam Structures with a Negative Poisson's Ratio. Science. 235(1987): 1038-1040.

[12] R.S. Lakes. Design Consideration for Materials with Negative Poisson's Ratios. Journal of Mechanical Design. 115(1993): 696-700.

[13] R.S. Lakes, K. Elms. Indentability of Conventional and Negative Poisson's Ratio Foams. Journal of Composite Materials. 27(1993): 1193-1202.

[14] M. Bianchi, F.L. Scarpa. Stiffness and energy dissipation in polyurethane auxetic foams. Journal of Materials Science. 43(2008): 5851-5860.

[15] A. Bezazi, F. Scarpa. Mechanical behaviour of conventional and negative Poisson's ratio thermoplastic polyurethane foams under compressive cyclic loading. International Journal of Fatigue. 29(2007): 922-930.

[16] A Bezazi, F. Scarpa. Tensile fatigue of conventional and negative Poisson's ratio open-cell PU foams. International Journal of Fatigue. 31(2009): 488-494.

[17] R. Lakes. Advances in negative Poisson's ratio materials. Advanced Materials. 5(1993): 293-296.

[18] L. Yang, D. Cormier, H. West, K. Knowlson. Non-stochastic Ti6Al4V foam structure that shows negative Poisson's Ratios. Materials Science and Engineering A. 558(2012): 579-585.

[19] L. Yang, O. Harrysson, D. Cormier, H. West. Compressive properties of Ti6Al4V auxetic mesh structures made by EBM process. Acta Materialia. 60(2012): 3370-3379.

[20] L. Yang, O. Harrysson, D. Cormier, H. West. Modeling of the uniaxial compression of 3D periodic re-entrant honeycomb structure. Journal of Materials Science. 48(2012): 1413-1422.

[21] Li Yang, Ola Harrysson, Harvey West, Denis Cormier. Mechanical properties of 3D re-entrant honeycomb structure: I- Modeling. Draft. 2013.

[22] Li Yang, Ola Harrysson, Harvey West, Denis Cormier. Mechanical properties of 3D re-entrant honeycomb structure: II – Experiments and discussion. Draft. 2013.

[23] L.J. Gibson. Cellular solids: structure and properties, 2nd edition. Cambridge University Press, New York, US, 1997.

[24] S. Webb, K. Peters, M.A. Zirky, T. Vella, S. Chadderdon, R. Selfridge, S. Schultz. Impact induced damage assessment in composite laminates through embedded fiber Bragg gratings, Smart Sensor Phenomena, Technology, Networks, and System 2010, Proceedings of SPIE. SPIE, San Diego, CA, 2010: 1-7.